Data in brief 26 (2019) 104495

Contents lists available at ScienceDirect

Data in brief

journal homepage: www.elsevier.com/locate/dib

Data Article

Data on the catalytic CO oxidation and CO_2 reduction durability on gC_3N_4 nanotubes Co-doped atomically with Pd and Cu

Kamel Eid, Aboubakr M. Abdullah*

Center for Advanced Materials, Qatar University, P.O. Box 2713, Doha, Qatar

ARTICLE INFO

Article history:
Received 1 July 2019
Received in revised form 27 August 2019
Accepted 2 September 2019
Available online 10 September 2019

Keywords:
CO_2 reduction
CO oxidation
Durability
Gas conversion reactions
One-dimensional gC_3N_4
Nanotubes

ABSTRACT

Understanding the fabrication mechanism of graphitic carbon nitride (gC_3N_4) nanostructures is critical for tailoring their physicochemical properties for various catalytic applications. In this article, we provide deep insights into the optimized parameters for the rational synthesis of one-dimensional gC_3N_4 atomically doped with Pd and Cu denoted as (Pd/Cu/gC_3N_4NTs) and its fabrication mechanism. This is in addition to the CO oxidation durability along with the electrochemical and photoelectrochemical CO_2 reduction durability of Pd/Cu/gC_3N_4NTs. The presented herein results are correlated to the research article entitled "Precise Fabrication of Porous One-dimensional gC_3N_4 Nanotubes Doped with Pd and Cu Atoms for Efficient CO Oxidation and CO_2 Reduction (Kamel Eid et al., 2019).

DOI of original article: https://doi.org/10.1016/j.inoche.2019.107460.
* Corresponding author.
E-mail address: bakr@qu.edu.qa (A.M. Abdullah).

https://doi.org/10.1016/j.dib.2019.104495

Specifications Table

Subject area	Chemistry
More specific subject area	Catalysis
Type of data	Scheme, Images, Table, and Figures
How data was acquired	Transmission electron microscope ((TEM), TecnaiG220, FEI, Hillsboro, OR, USA), scanning electron microscope ((SEM), Hitachi S-4800, Hitachi, Tokyo, Japan), X-ray diffraction patterns ((XRD), X'Pert-Pro MPD, PANalytical Co., Almelo, Netherlands), CO oxidation (online gas analyzer IR-200, Yokogawa, Japan), CO_2 reduction Gamry electrochemical analyzer (reference 3000, Gamry Co., USA).
Data format	The obtained data are imaged and analyzed.
Experimental factors	The thermal CO oxidation stability tests were measured under continuous gas mixture flow while heating (25−300 °C). The electrocatalytic CO_2 reduction durability tests were benchmarked at the room temperature in 0.5 M $NaHCO_3$ solution.
Experimental features	Changing the reaction parameters and conditions to optimizing the fabrication process of Pd/Cu/gC_3N_4. Investigation the thermal CO oxidation durability as well as the electrochemical and photoelectrochemical CO_2 reduction of Pd/Cu/gC_3N_4. These results are beside the structural and compositional analysis of Pd/Cu/gC_3N_4 after the catalytic durability reactions.
Data source location	Center for advanced materials, Qatar University, Doha 2713, Qatar.
Data accessibility	The data are obtained and provided in this article.
Related research article	Eid et al., Precise Fabrication of Porous One-dimensional gC_3N_4 Nanotubes Doped with Pd and Cu Atoms for Efficient CO Oxidation and CO_2 Reduction, *Inorganic Chemistry Communications*." [1]

Value of the data

- Optimization of the fabrication process of gC_3N_4 nanostructures doped with binary metals is essential in various catalytic applications.
- Understanding the fabrication mechanism of Pd/Cu/gC_3N_4NTs is essential for tailoring their physicochemical and catalytic properties for various applications.
- The catalytic CO oxidation and CO_2 reduction durability of Pd/Cu/gC_3N_4NTs are central factors in commercial applications.
- These data may open new avenues on using gC_3N_4-based materials for gas conversion reactions.

1. Data

The presented data article is associated with the research article (Kamel Eid et al., 2019 [1]). This includes (i) the SEM and TEM images of metal-free gC_3N_4, (ii) the TEM images of Pd/Cu/gC_3N_4 prepared in different morphologies, (iii) the CO oxidation durability of Pd/Cu/gC_3N_4NTs, Pd/gC_3N_4NTs, and Cu/gC_3N_4NTs, (iv) the electrocatalytic and photoelectrochemical CO_2 reduction of Pd/Cu/gC_3N_4NTs, and (v) the XRD, EDX, and TEM image of Pd/Cu/gC_3N_4 after the CO durability testes.

2. Experimental design, materials, and methods

2.1. CO oxidation

We tested the CO oxidation reaction in a fixed bed quartz tubular reactor connected to an online gas analyzer (IR200, Yokogawa, Japan) in the presence of 50 mg of each catalyst. Initial pretreatment was carried out at 250 °C under an O_2 flow of 50 mL min^{-1} for 1 h, and then H_2 (30 mL min^{-1}) for 1 h. Following that, the catalysts were exposed to the gas mixture involving of 4% CO, 20% O_2, and 76% Ar with a total flow of 50 mL min^{-1} under continuous heating from 25 °C to 400 °C (5°min^{-1}) [1–5]. The percentage of CO conversion (% CO) was calculated using the following equation:

$$\%CO = [(CO_{in} - CO_{out})] / CO_{in} \times 100 \quad (1)$$

where CO_{in} is, the input quantity and CO_{Out} is the output quantity.

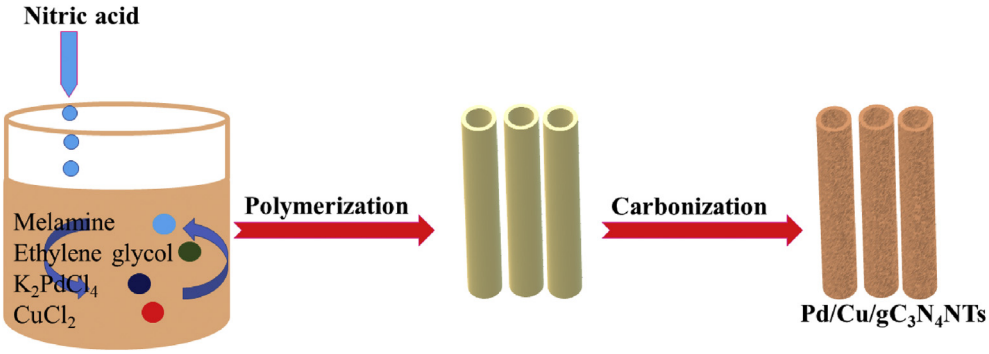

Scheme 1. Schematic shows the synthesis process of Pd/Cu/gC_3N_4NTs.

2.2. Electrochemical reduction of CO_2

The cyclic voltammogram (CVs), linear sweep voltammogram (LSV), and electrochemical impedance spectroscopy (EIS) measurements were measured on Gamry electrochemical analyzer (reference 3000, Gamry Co., USA) using a three-electrode system composed of a Pt wire (counter electrode), Ag/AgCl (reference electrode), and glassy carbon ((5mm) working electrode). The CVs, LSVs, and EIS were measured in a CO_2-saturated aqueous solution of 0.5 M $NaHCO_3$ at a sweep rate of 50 mV s^{-1}. In the photoelectrochemical measurements, the light source was ozone-free xenon lamp (100 W, Abet Technologies, USA) with fluorine-doped tin oxide as a working electrode in a Quartz photo-glass cell (50 mm × 50 mm). The catalyst loading amount of each catalyst on the working electrode was fixed to 10 μg cm^{-2} using. After deposition of each catalyst on the working electrodes, a 5 μL of Nafion solution (1 wt %) was added on each electrode and left to dry completely under vacuum at 80 °C before the measurements.

Scheme 1 shows the fabrication process of Pd/Cu/gC_3N_4NTs, including the initial slow mixing of melamine in an aqueous solution of ethylene glycol solution, contains Pd- and Cu precursors [3]. Then, nitric acid was added dropwise to slowly deprotonate melamine and facilities the polymerization step

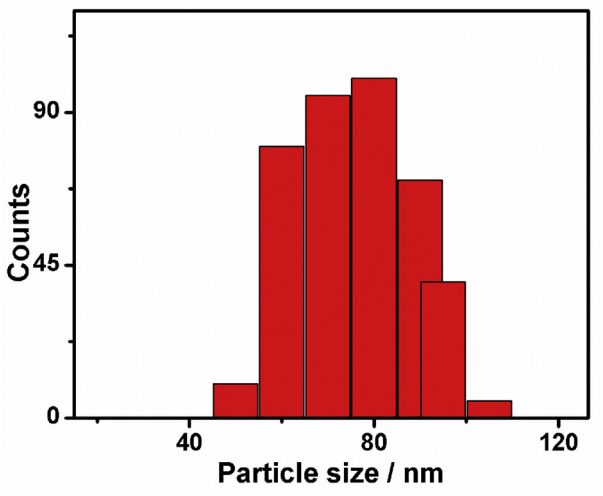

Fig. 1. The size distribution histogram of Pd/Cu/gC_3N_4NTs.

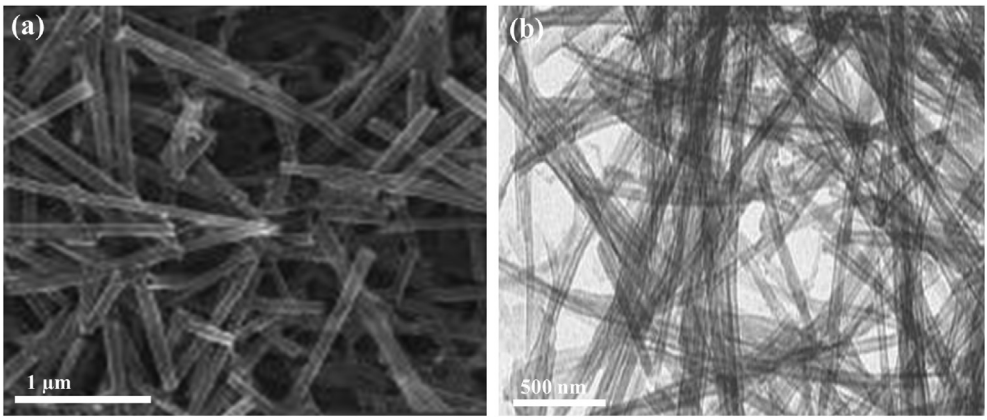

Fig. 2. (a) SEM and (b) TEM images of gC_3N_4NTs.

to polymeric gC_3N_4, followed by annealing at elevated temperature to allow the carbonization process and formation of gC_3N_4NTs doped with Pd and Cu.

Fig. 1 shows the histogram chart of Pd/Cu/gC_3N_4NTs. The widths of thus obtained Pd/Cu/gC_3N_4NTs ranged from 60 to 90 nm. The average width of thus formed nanotubes is nearly 80 nm.

Fig. 2 shows the SEM and TEM images of metal-free gC_3N_4NTs that were prepared by the same method of Pd/Cu/gC_3N_4NTs but in the absence of Pd and Cu precursors. Fig. 2a reveals the SEM image of gC_3N_4NTs formed in high yield (nearly 100%) of nanotubes shape. The nanotube shape was uniform and mono distributed with an average width of 78 nm and an average length of 1.4 μm. The TEM image shows the absence of any undesired nanostructures such as spherical nanoparticles or other shapes.

2.3. Fabrication parameters optimization

Fig. 3a shows the TEM image of Pd/Cu/C_3N_4NTs nanoflakes prepared by the quick mixing of melamine (1 g) in an aqueous solution of ethylene glycol solution (30 mL) involving K_2PdCl_4 (20 mM) and $CuCl_2$ (20 mM) followed by the slow addition of HNO_3 (60 mL of 0.1 M) under stirring. The obtained precipitate was washed with ethanol and dried at 80 °C for 12 h before annealing at 550 °C (5 °C/min) for 2 h under nitrogen. The TEM image reveals the formation of aggregated flakes-like Pd/Cu/C_3N_4NTs nanostructures obtained in a high yield with an average dimension of ~ 250 nm.

Under the same conditions and parameters of nanoflakes, the quick addition of nitric acid produced sheet-like nanostructures. This arose from the quick deprotonation and polymerization process via rapid addition of nitric acid (Fig. 3b). Reducing the concertation of nitric acid to 0.03 M with fixing all other conditions and parameters formed aggregated and non-uniform Pd/Cu/C_3N_4 nanotubes (Fig. 3c). Using isopropanol solution instated of ethylene glycol led to the production of Pd/Cu/C_3N_4 nanofibers in line with our previous reports (Fig. 3d) [2]. The as-formed nanofibers were highly uniform with average dimensions of 1.5 ± 0.2 μm in length and 80 ± 3 nm in width.

Fig. 3e shows the formation of gC_3N_4 nanosheets decorated with aggregated Pd/Cu nanoparticles formed through increasing the concertation of Pd/Cu to 60 mM instead of 20 mM with fixing all other conditions. Similarly, decreasing the concertation of Pd/Cu to 40 mM drove the formation of nanosheets decorated with uniform Pd/Cu nanoparticles (Fig. 3f). These results warranted that the formation of Pd/Cu/C_3N_4NTs is highly sensitive to the concentration of reactants and their mixing conditions. In particular, the addition of melamine and nitric acid should be sluggish to provide enough time for a consistent polymerization into uniform nanotubes. Nitric acid facilitates the deprotonation of active $-NH_2$ groups of melamine and allowing the conversion of melamine into melem and then to polymeric gC_3N_4 composed of triazine-based units after carbonization at an elevated temperature [1–5]. Meanwhile, the concertation of Pd/Cu precursors should be lower to be anchored on the N-

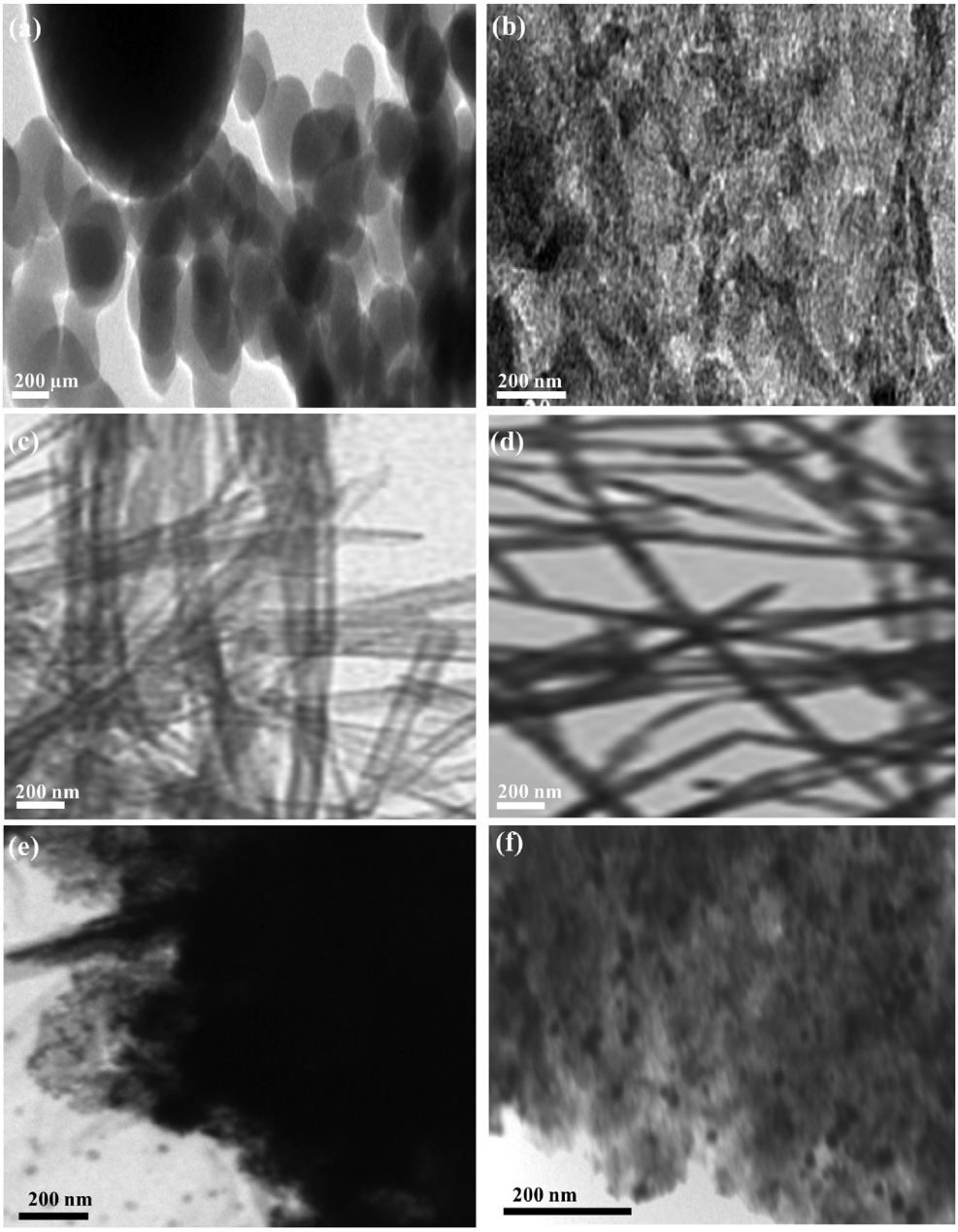

Fig. 3. (a) TEM images of Pd/Cu/gC_3N_4NTs obtained by (a) quick addition of melamine, (b) quick addition of HNO_3, (c) using 60 mL of HNO_3 (0.03 M), (d) using ethanol instead of ethylene glycol. (e) Pd/Cu/gC_3N_4NTs formed using 60 mM of K_2PdCl_4 and $CuCl_2$ and (f) using 40 mM of K_2PdCl_4 and $CuCl_2$.

atoms of melamine and then facilitating the atomic doping of Pd/Cu instead of formation of nanoparticles [1–5]. On the other hand, glycol-mediated solution acting as a structure-directing agent for driving the formation of nanotube shape.

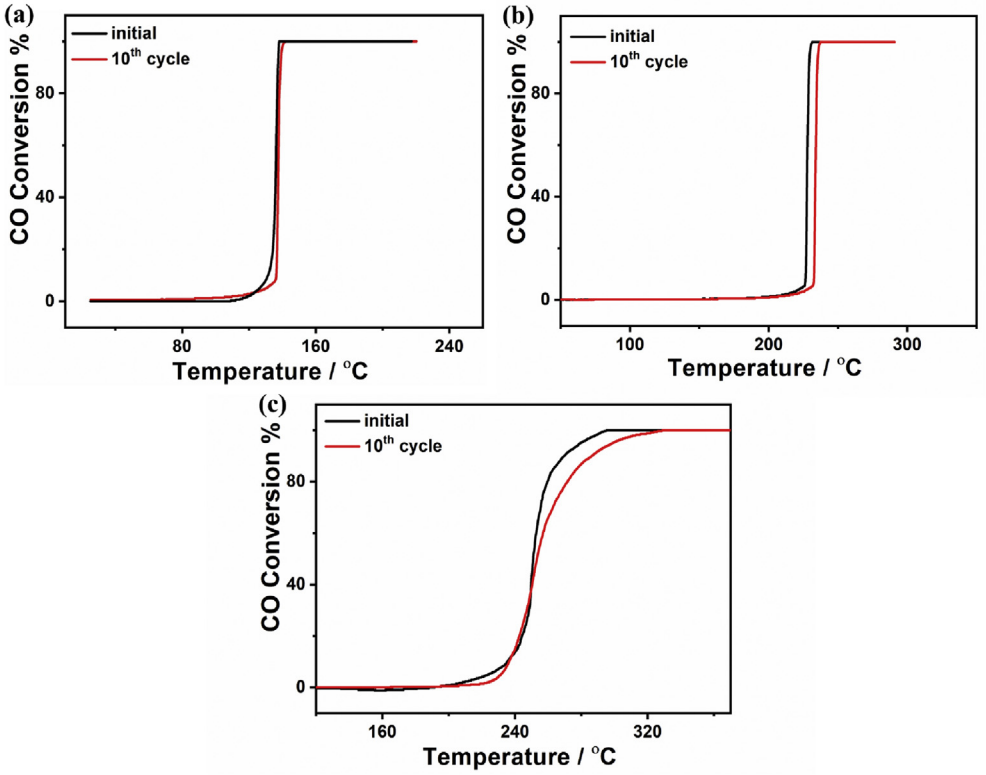

Fig. 4. The CO oxidation light-off stability tests measured on (a) Pd/Cu/gC_3N_4NTs, (b) Pd/gC_3N_4NTs, and (c) Cu/gC_3N_4NTs for ten cycles at their T_{100}.

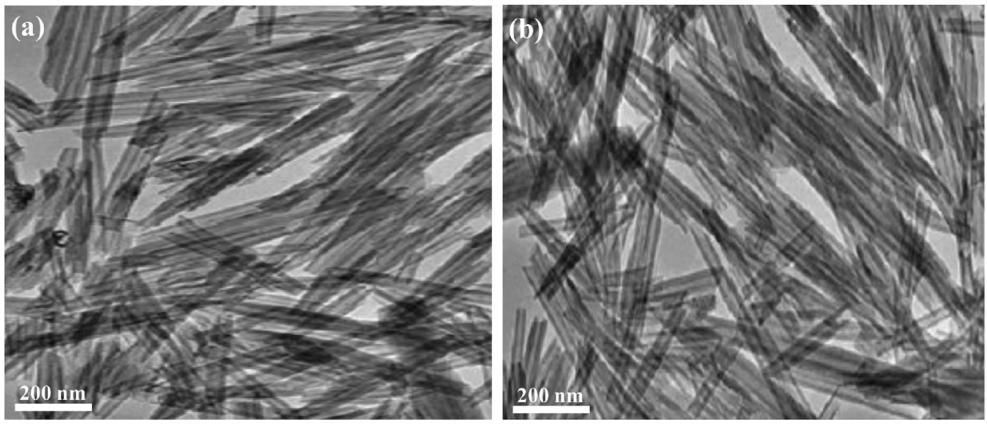

Fig. 5. The TEM image of Pd/Cu/gC_3N_4NTs before (a) and after (b) the stability tests.

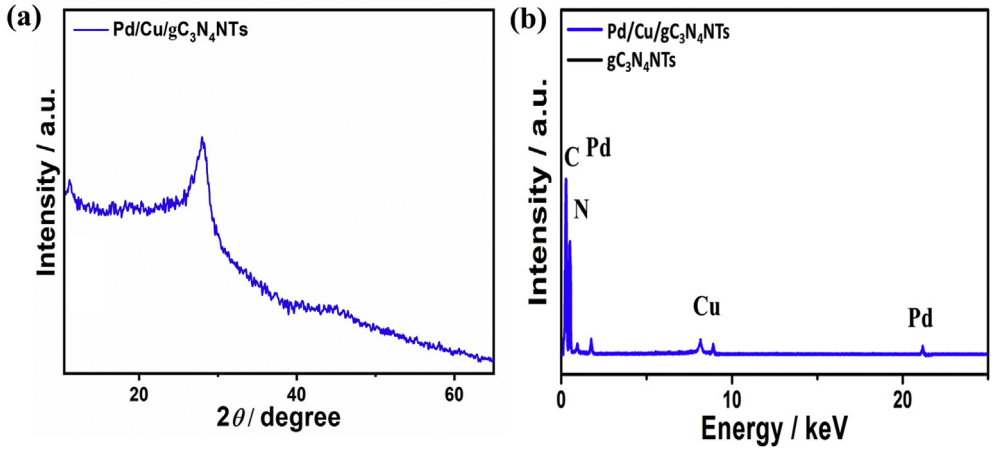

Fig. 6. (a) XRD analysis and (b) EDX analysis of Pd/Cu/gC_3N_4NTs after the CO durability tests.

2.4. CO oxidation stability tests

The CO oxidation durability is an important factor in large-scale environmental and industrial applications [1–4]. Fig. 4 shows the accelerated durability tests of Pd/Cu/gC_3N_4NTs, Pd/gC_3N_4NTs, and Cu/gC_3N_4NTs measured for ten cycles at their complete CO conversion temperature (T_{100}). The results show that Pd/Cu/gC_3N_4NTs is more durable than both Pd/gC_3N_4NTs and Cu/gC_3N_4NTs. Particularly, the CO oxidation kinetics and T_{100} of Pd/Cu/gC_3N_4NTs were almost maintained without any significant changes (Fig. 4a). Meanwhile, the T_{100} of Pd/gC_3N_4NTs, and Cu/gC_3N_4NTs increased only by around 11 °C (Fig. 4b) and 25 °C (Fig. 4c), respectively. However, the CO oxidation kinetics did not decrease substantially on both Pd/gC_3N_4NTs and Cu/gC_3N_4NTs, as shown in their light-off curves (Fig. 4b and c).

The sample was dispersed in ethanol and sonicated for 3 min and then mounted on a carbon-coated TEM grid. Fig. 5 reveals the TEM images of Pd/Cu/gC_3N_4NTs before (Fig. 5a) and after the CO oxidation stability tets (Fig. 5b). Comparing the TEM image of Pd/Cu/gC_3N_4NTs before and after the CO oxidation durability testes, we found that the structural stability of nanotube shape is fully maintained without any changes. Therefore, the nanotube morphology did not change after ten durability cycles.

Fig. 6a shows the XRD analysis of Pd/Cu/gC_3N_4NTs after the CO durability tests, which displayed the one diffraction peak at 27.01° assigned to {002} facet and one peak at 13.15° attributes to{100} facet of gC_3N_4 nanostructure similar to those obtained for Pd/Cu/gC_3N_4NTs before the CO durability tests. Thus,

Table 1
Comparison between the CO oxidation activity of our newly designed Pd/Cu/gC_3N_4NTs and various catalysts reported elsewhere.

Catalyst	Complete CO conversion, T_{100}	Reference
Pd/Cu/gC_3N_4NTs	154 °C	Our work
$Au_{0.75}Cu_{0.25}/SiO_2$	300 °C	[6] *Catal. Today*, 2017, 282 105–110.
Pd/La-doped γ-alumina	175 °C	[7] *Nat. Commun.*, 2014, *5*, 4885.
Pd-impeded 3D porous graphene	190 °C	[8] *ACS Nano* 2015, 9, 7343-7351
Pt/CNx/SBA-15	250 °C	[9] *Chem. A Eur. J.*, 2014, 20, 2872–2878.
Nanoarray-based $CuMn_2O_4$/Washed-coated $CuMn_2O_4$	320 °C/350 °C	[10] *J. Mater. Chem. A*, 2018, 6, 19047-19057
Cu_1/Mn_1	180 °C	[11] *Catal. Lett.*, 2016, 146, 2364-2375
MnO_x	310 °C	[12] *Catal. Sci. Technol.*, 2016, 6, 8222-8233

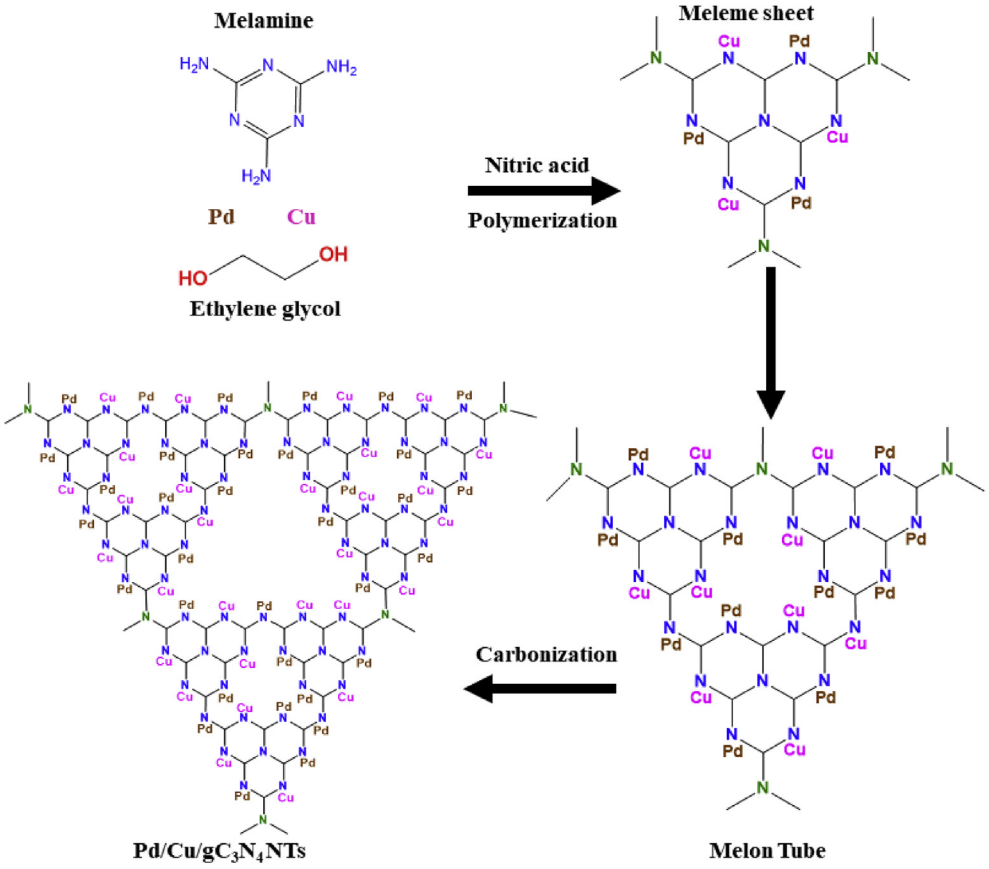

Scheme 2. The formation mechanism of Pd/Cu/gC_3N_4NTs and the distribution of Pd and Cu inside gC_3N_4NTs.

the XRD result indicates that Pd/Cu/gC_3N_4NTs reserved its crystallinity after the CO oxidation durability tests. The EDX analyses after CO stability testes is carried out to confirm the compositional durability of Pd/Cu/gC_3N_4NTs (Fig. 6b). The results showed the presence of C, N, Pd, and Cu with atomic contents of 58, 40.9, 0.5, and 0.6, respectively (Fig. 6b). Thus, the EDX result implies that Pd/Cu/gC_3N_4NTs kept its composition without any deterioration, owing to the homogenous distribution of Pd and Cu inside the carbon matrix.

Table 1 shows the comparison between the catalytic CO oxidation activity of our newly designed Pd/Cu/gC_3N_4NTs and the previously reported catalysts such as Pd-based, Au-based Cu-based, Pt-based, and Mn-based. The complete conversion temperature of our obtained Pd/Cu/gC_3N_4NTs was significantly lower than that of all the catalysts reported in the literature as shwon in Table 1 in addition to the low cost of our catalyst that was made of nearly 99% gC_3N_4NTs and 1% Pd/Cu.

The TEM, XRD, and EDX results confirmed the structural and compositional stability of the as-synthesized Pd/Cu/gC_3N_4NTs after the CO oxidation stability tests. This probably originates from coupling between the unique physicochemical properties of 1D gC_3N_4 nanotubes (e.g., stability, massive accessible active sites, thermal stability nearly up to 600 °C, and chemical stability in various solvents) and the inherent catalytic merits of Pd/Cu (eg., electronic effect, synergetic effect, strong adsorption/activation/dissociation for CO/O_2, and high tolerance for CO_2 product) [1–5,13–16]. Chemically speaking, the atomic doping of gC_3N_4NTs with Pd and Cu stabilizes them against aggregation as well as protecting their active catalytic sites from the blocking by the reaction intermediates or products.

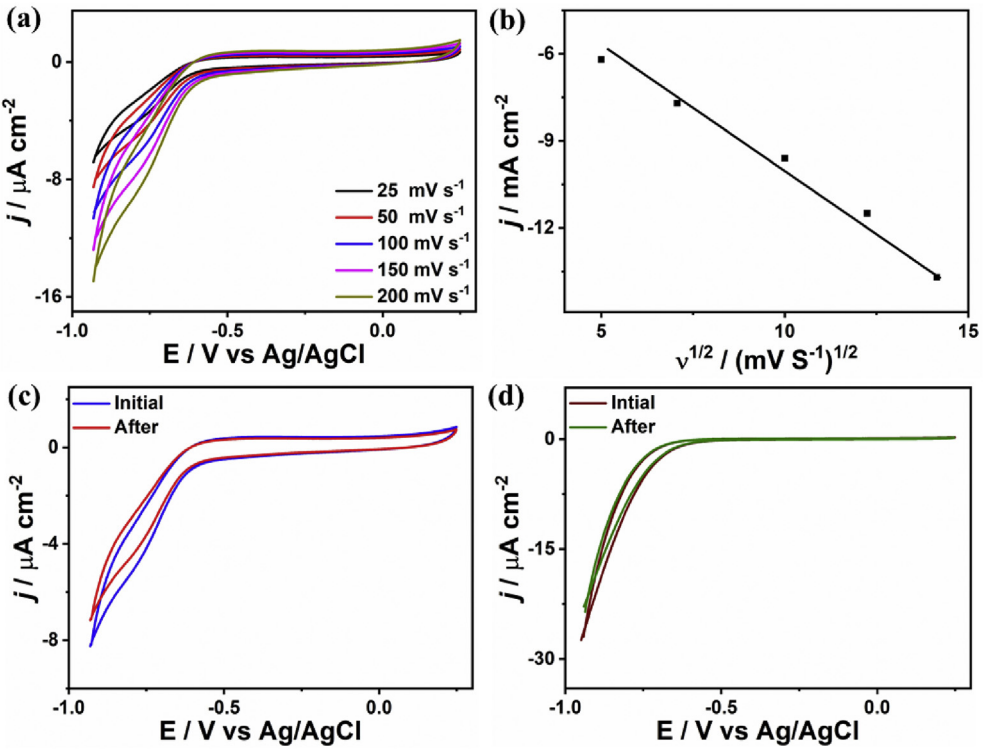

Fig. 7. (a) The CVs measured on the as-made catalysts in CO_2-saturated 0.5 $NaHCO_3$ at 50 mV s^{-1} under different scan rates and (b) Randles-Sevcik equation. (c) The electrochemical CVs durability on Pd/Cu/gC_3N_4NTs measured under dark. (d) The photo-electrochemical CVs stability tested under continuous light irradiation (100 W). We performed all the measurements at the room temperature.

Scheme 2 shows the formation process and mechanism of typically prepared Pd/Cu/gC_3N_4. The strong binding affinity between N-atoms of melamine and Pd/Cu facilitate adsorption and anchoring of both Pd and Cu on N-atoms during the polymerization step that led to the homogenous atomic distribution of Pd, and Cu on the N-atoms of gC_3N_4.

Fig. 7a shows the CVs for CO_2 reduction measured under various sweeping rates ranged from 25 to 200 mV s^{-1}, which showed the steady enhancement in the current density with increasing the scan rate. The relationship between the obtained current densities and the square root of scan rates is linear (Fig. 7b).

The electrocatalytic and photo-electrochemical CO_2 reduction durability tests were carried out on Pd/Cu/gC_3N_4NTs via measuring the chronoamperometric test (*I-T*) for 30 min in CO_2-saturated an aqueous solution of 0.5 $NaHCO_3$ at 50 mV s^{-1}. Then the CVs curve were measured again in CO_2-saturated an aqueous solution of 0.5 $NaHCO_3$ at 50 mV s^{-1}. The CVs curves showed that Pd/Cu/gC_3N_4NTs kept its initial electrocatalytic CO_2 reduction activity (Fig. 7c) without any significant deterioration in the current density, reduction kinetics, and reduction potential (Fig. 7d), [17].

Fig. 8 depicts the gas chromatography result that was obtained after calibration relative to pure formic acid and methanol under the same conditions. The results demonstrated the presence of formic acid as the main product as well as methanol as an inferior product (Fig. 8). Therefore, the gas chromatography indicates the ability of Pd/Cu/gC_3N_4NTs to reduce CO_2 electrochemically to formic acid at room temperature.

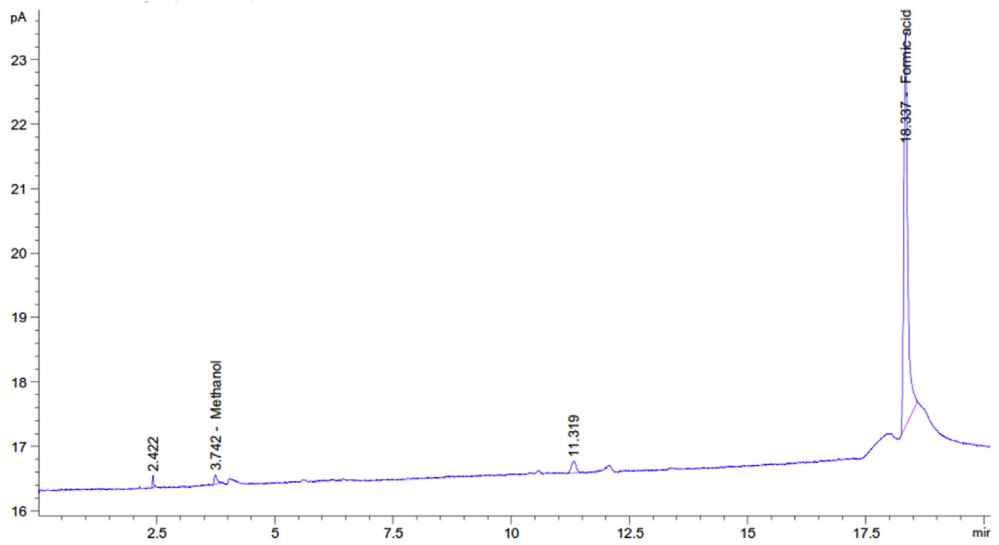

Fig. 8. CO_2 reduction products obtained from the Gas chromatography (Agilent Technologies 7890A) with using a column PerkinElmer Elite-624 at 35 °C.

Acknowledgments

This publication was supported by Qatar university Grant No. IRCC 179. The findings achieved herein are solely the responsibility of the authors.

Conflict of interest

The authors declare that they have no known competing financial interests or personal relationships that could have appeared to influence the work reported in this paper.

Appendix A. Supplementary data

Supplementary data to this article can be found online at https://doi.org/10.1016/j.dib.2019.104495.

References

[1] K. Eid, M.H. Sliem, S.Y. Al-Qaradawi, A.M. Abdullah, Precise fabrication of porous one-dimensional gC_3N_4 nanotubes doped with Pd and Cu atoms for efficient CO oxidation and CO_2 reduction, Inorg. Chem. Commun. 107 (2019), 107460.
[2] K. Eid, M.H. Sliem, A.S. Eldesoky, H. Al-Kandari, A.M. Abdullah, Rational synthesis of one-dimensional carbon nitride-based nanofibers atomically doped with Au/Pd for efficient carbon monoxide oxidation, Int. J. Hydrogen Energy 44 (2019) 17943–17953.
[3] K. Eid, M.H. Sliem, H. Al-Kandari, M.A. Sharaf, A.M. Abdullah, Rational synthesis of porous graphitic-like carbon nitride nanotubes codoped with Au and Pd as an efficient catalyst for carbon monoxide oxidation, Langmuir 35 (2019) 3421–3431.
[4] K. Eid, H.Y. Ahmad, T.A. Mohamed, G.A. Elsafy, Y.S. Al-Qaradawi, Versatile synthesis of Pd and Cu Co-doped porous carbon nitride nanowires for catalytic CO oxidation reaction, Catalysts (2018) 8.
[5] K. Eid, M.H. Sliem, A.M. Abdullah, Unraveling template-free fabrication of carbon nitride nanorods codoped with Pt and Pd for efficient electrochemical and photoelectrochemical carbon monoxide oxidation at room temperature, Nanoscale 11 (2019) 11755–11764.
[6] P. Destro, S. Marras, L. Manna, M. Colombo, D. Zanchet, AuCu alloy nanoparticles supported on SiO_2: impact of redox pretreatments in the catalyst performance in CO oxidation, Catal. Today 282 (2017) 105–110.
[7] E.J. Peterson, A.T. DeLaRiva, S. Lin, R.S. Johnson, H. Guo, J.T. Miller, J. Hun Kwak, C.H.F. Peden, B. Kiefer, L.F. Allard, F.H. Ribeiro, A.K. Datye, Low-temperature carbon monoxide oxidation catalysed by regenerable atomically dispersed palladium on alumina, Nat. Commun. 5 (2014) 4885.

[8] R. Kumar, J.-H. Oh, H.-J. Kim, J.-H. Jung, C.-H. Jung, W.G. Hong, H.-J. Kim, J.-Y. Park, I.-K. Oh, Nanohole-structured and palladium-embedded 3D porous graphene for ultrahigh hydrogen storage and CO oxidation multifunctionalities, ACS Nano 9 (2015) 7343–7351.
[9] P. Xiao, Y. Zhao, T. Wang, Y. Zhan, H. Wang, J. Li, A. Thomas, J. Zhu, Polymeric carbon nitride/mesoporous silica composites as catalyst support for Au and Pt nanoparticles, Chem. Eur J. 20 (2014) 2872–2878.
[10] S.-Y. Chen, W. Tang, J. He, R. Miao, H.-J. Lin, W. Song, S. Wang, P.-X. Gao, Steven L. Suib, Copper manganese oxide enhanced nanoarray-based monolithic catalysts for hydrocarbon oxidation, J. Mater. Chem. 6 (2018) 19047–19057.
[11] Y. Guo, J. Lin, C. Li, S. Lu, C. Zhao, Copper manganese oxides supported on multi-walled carbon nanotubes as an efficient catalyst for low temperature CO oxidation, Catal. Lett. 146 (2016) 2364–2375.
[12] Y. Xie, Y. Guo, Y. Guo, L. Wang, W. Zhan, Y. Wang, X.-q. Gong, G. Lu, A highly-efficient La-MnOx catalyst for propane combustion: the promotional role of La and the effect of the preparation method, Catal. Sci. Technol. 6 (2016) 8222–8233.
[13] J. Barrio, L. Lin, P. Amo-Ochoa, J. Tzadikov, G. Peng, J. Sun, F. Zamora, X. Wang, M. Shalom, Unprecedented centimeter-long carbon nitride needles: synthesis, characterization and applications, Small 14 (2018), 1800633.
[14] J. Xu, T. White, P. Li, C. He, J. Yu, W. Yuan, Y.-F. Han, Biphasic Pd-Au alloy catalyst for low-temperature CO oxidation, J. Am. Chem. Soc. 132 (2010) 10398–10406.
[15] C. Han, Y. Gao, S. Liu, L. Ge, N. Xiao, D. Dai, B. Xu, C. Chen, Facile synthesis of AuPd/g-C_3N_4 nanocomposite: an effective strategy to enhance photocatalytic hydrogen evolution activity, Int. J. Hydrogen Energy 42 (2017) 22765–22775.
[16] M. Inagaki, T. Tsumura, T. Kinumoto, M. Toyoda, Graphitic carbon nitrides (g-C_3N_4) with comparative discussion to carbon materials, Carbon 141 (2019) 580–607.
[17] L. He, M. Fei, J. Chen, Y. Tian, Y. Jiang, Y. Huang, K. Xu, J. Hu, Z. Zhao, Q. Zhang, H. Ni, L. Chen, Dataset of emission and excitation spectra, UV-vis absorption spectra, and XPS spectra of graphitic C_3N_4, Data in Brief 21 (2018) 501–510.